

Harnessing the Benefits of PEDOT:PSS Conductive Coating for Prolonged Cycle Life of Copper Hexacyanoferrate in Aqueous Zinc-Ion Batteries

Mohsen Baghodrat,^[a] Jens Glenneberg,^[b] Giorgia Zampardi,*^[a] and Fabio La Mantia*^[a, b]

The utilization of copper hexacyanoferrate (CuHCF) as positive electrode material in aqueous zinc-ion batteries (ZIBs) has gained significant attention due to its efficient (de-)intercalation of Zn^{2+} ions, cost-effective synthesis, low toxicity, and high working potential. One approach to improve its electrochemical performance is to coat the CuHCF particles with conductive polymers, such as poly(3,4-ethylenedioxythiophene): polystyrene sulfonate (PEDOT:PSS). In this study, we investigated the impact of the PEDOT:PSS as a coating on the electrochemical behavior and the cycle life of CuHCF for aqueous ZIB applications. Galvanostatic cycling performed at a

current rate of 1 C relevant for the stationary application of the CuHCF/PEDOT:PSS electrodes having high mass loadings (10 mg cm^{-2} of active material) revealed significantly longer cycle life while maintaining a high Coulombic efficiency ($\geq 99.5\%$). The longest cycle life was achieved with CuHCF coated using a 4.5 wt.% PEDOT:PSS aqueous coating dispersion. These findings demonstrate the potential of conductive polymer coatings as a practical approach to enhance the electrochemical performance of positive electrode materials in aqueous Zinc-ion batteries.

1. Introduction

The development of sustainable energy storage technologies is of utmost importance in view of the current efforts to reduce our carbon footprint and to create a greener future. With the growing demand for eco-friendly energy solutions, aqueous zinc-ion batteries (A-ZIBs) have emerged as a potential alternative to conventional lithium-ion batteries in grid energy storage systems.^[1,2] A-ZIBs offer potential benefits in terms of low cost, high specific power, and low environmental impact. However, their commercial viability has yet to be achieved due to challenges in finding a suitable Zn-insertion material for the positive electrode that is non-toxic, cost-effective, and durable when cycled in aqueous electrolytes.^[3–5]

Hexacyanometallates of transition metals, commonly referred to as Prussian blue analogues (PBAs), have garnered significant attention as potential positive electrode materials in aqueous ZIBs. PBAs offer several advantages, including low toxicity, low cost, and high reversibility toward (de-)inserting

various cations while maintaining minimal structural volume changes.^[4,6,7]

Copper hexacyanoferrate (CuHCF) is a type of PBA that has gained attention as a positive electrode material in A-ZIBs due to its high reversibility towards the insertion of Zn^{2+} , high power rate capability, and high cell working potential. This material can be synthesized using abundant, non-toxic elements through a simple, low-cost synthesis process that can be easily scaled up at industrial levels. With its high cell working potential of about 1.7 V vs. Zn^{2+}/Zn , CuHCF-based aqueous ZIBs have the ability to fully utilize the electrochemical stability window of water.^[8–16] Despite its advantages, however, CuHCF is challenged by its relatively short cycle life in rechargeable aqueous Zn-ion batteries compared to the commercial insertion materials used in organic Li-ion batteries.^[8,17–19]

The coordination chemistry of CuHCF provides flexible means for refining its electrochemical performance and durability by changing its synthesis conditions, such as reaction time, reaction temperature, reactant concentrations, and/or thermal treatment. These modifications impact, for example, the positioning of the elements, the potassium or iron content, and the amount of coordinated water in the CuHCF lattice.^[13,15,20–22] However, although the stability and the electrochemical properties of CuHCF can be improved by altering its synthesis settings, finding the optimal route remains challenging.

One straightforward approach to enhance the electrochemical performance and, in particular, to overcome the cycle life limitations is using conductive polymers as a coating on the active materials. Conductive polymer coatings usually act as mediators for transferring ions and electrons, leading to improved rate capability and power density. Moreover, they act as a protective barrier that reduces the active material's

[a] M. Baghodrat, Dr. G. Zampardi, Prof. Dr. F. La Mantia
Universität Bremen, Energiespeicher-und Energiewandlersysteme, Bibliothekstraße 1, 28359 Bremen, Germany
E-mail: zampardi@uni-bremen.de
lamantia@uni-bremen.de

[b] Dr. J. Glenneberg, Prof. Dr. F. La Mantia
Fraunhofer Institute for Manufacturing Technology and Advanced Materials – IFAM, Wiener Straße 12, 28359 Bremen, Germany

Supporting information for this article is available on the WWW under <https://doi.org/10.1002/batt.202400156>

© 2024 The Authors. *Batteries & Supercaps* published by Wiley-VCH GmbH. This is an open access article under the terms of the Creative Commons Attribution Non-Commercial NoDerivs License, which permits use and distribution in any medium, provided the original work is properly cited, the use is non-commercial and no modifications or adaptations are made.

degradation or dissolution rate and mitigates the side reactions, thus prolonging the battery's cycle life.^[23–29]

Different types of conductive polymers can be synthesized to tailor their physicochemical and mechanical properties depending on the application, for example, by varying dopants levels, molecular weights, and degrees of crosslinking. This makes conductive polymer coatings suitable for use in a wide range of energy storage applications, from small-scale consumer electronics to large-scale grid energy storage systems.^[23,24,26,29–38]

Among the various conductive polymers, poly(3,4-ethylenedioxythiophene): polystyrene sulfonate (PEDOT:PSS), has interesting properties making it a good candidate as a coating for Prussian blue analogues materials. Indeed, PEDOT:PSS is a combination of positively charged conjugated PEDOT and negatively charged saturated PSS that work together to provide electrical conductivity and electrochemical stability. It is a solution-processable, high-performance conductive polymer developed for various applications, including batteries, displays, and sensors.^[6,39–47] PEDOT is a conjugated polymer well known for its high electrical conductivity, which makes it a suitable choice for battery use. However, the material is not easily dispersible and has a limited electrochemical stability window,^[48–51] hindering its effectiveness in aqueous metal-ion batteries. The addition of the PSS component helps to overcome these limitations since PSS is a polymer surfactant whose presence improves the dispersion and the stability of PEDOT in water and other solvents.^[6,30,41,52] It has been shown that the combination of the two polymers (PEDOT:PSS) is highly resistant to electrochemical degradation, and it maintains its conductive properties over a wide range of temperatures and humidity.^[27,39,42,43,45,47,53,54] This makes PEDOT:PSS an ideal choice in demanding environments and potentially an effective coating material for CuHCF in aqueous ZIBs.

In particular, PEDOT:PSS has recently been proposed as a coating/additive at the solid state to enhance the electrochemical performance of positive electrodes based on Prussian blue and its analogues. For example, Kim et al.^[6] used different amounts of PEDOT:PSS mixed with Prussian blue particles, which resulted in different coating of the materials. It has been shown that the PEDOT:PSS coating on the surface of the Prussian blue particles improved their electrical conductivity when the material was used as a Na⁺-insertion cathode for organic Na-ion batteries. It was found that a small amount of PEDOT:PSS on the surface of the characteristic Prussian blue nanocubes formed a highly conductive network, which improved the reversible capacity and rate capability of the material over the cycles. A similar approach was followed by Xu et al.,^[41] who encapsulated Prussian blue nanocrystals with PEDOT:PSS while using ethylene glycol as a polar solvent in the coating polymer dispersion. This approach resulted in a further increased electrical conductivity of the Prussian blue particles encapsulated with the polymer. The resulting Prussian blue/PEDOT-PSS nanohybrid showed improved specific capacity, cyclability, and rate capability compared to the uncoated sample, making it a potential candidate for high-performance Li-ion batteries.

Despite the promising results in the field of organic-based Li- and Na-ion batteries, the application of PEDOT:PSS as a solid-state additive within the positive electrodes in aqueous ZIBs remains largely unexamined, especially in the case of PBAs cathode active materials. Moreover, the electrochemical properties of PBAs coated with PEDOT:PSS for aqueous ZIBs application remain still unexplored. Thus, within this study, the potential benefits of PEDOT:PSS as a solid-state additive/coating of CuHCF particles have been investigated. In order to do so, CuHCF particles have been synthesized in-house and coated with PEDOT:PSS. The compatibility between PEDOT:PSS and CuHCF and the electrochemical stability of PEDOT:PSS has been assessed in a mildly acidic environment and in the potential conditions dictated by the Zn²⁺ (de-)insertion in CuHCF. The effect of adding different amounts of PEDOT:PSS as a solid-state additive on the cycle life of CuHCF has been assessed through galvanostatic experiments conducted with high mass loading electrodes (10 mg cm⁻² of active material) at a current rate of 1 C, in order to align with the requirements imposed by the stationary application.^[2]

Experimental

Material Synthesis

The standard coprecipitation method outlined in reference^[15] was used to synthesize the uncoated CuHCF particles. Briefly, 50 mM Cu(NO₃)₂ • 3H₂O and 100 mM K₃Fe(CN)₆ (both from Sigma Aldrich) were added dropwise to 60 ml of deionized water with vigorous stirring, resulting in the immediate formation of a brown suspension. The suspension was then bath sonicated for 30 minutes and left to settle overnight. The precipitate was centrifuged and washed with a solution containing 1 M KNO₃ and 10 mM HNO₃ (both from Sigma Aldrich), followed by rinsing with deionized water in order to eliminate any remaining impurities or unreacted precursors from the synthesis. The material was then dried overnight at 60 °C, consequently ground using mortar and pestle. To coat CuHCF, 1 g of the obtained CuHCF powder was dispersed in 40 mL of deionized water and stirred for 24 h. Various amounts of a commercial PEDOT:PSS suspension (Clevios™ PH 1000, Heraeus Deutschland GmbH), containing 5 wt.% added dimethyl sulfoxide (DMSO, Sigma Aldrich), was poured into the dispersion and stirred for 72 h. The mixture was dried overnight at 60 °C and ground using a mortar and pestle to obtain the final coated powder, i.e., CuHCF@PEDOT:PSS. Finally, the obtained powder consisted 2.5, 4.5, 8.5, or 12.5 wt.% of PEDOT:PSS.

Material Characterization

The presence of PEDOT:PSS on the CuHCF particles was checked with the aid of scanning electron microscopy (SEM) coupled with energy-dispersive X-ray spectroscopy (EDS). The SEM images were acquired at different magnifications using a FEI Helios NanoLan 600 DualBeam® apparatus with an acceleration voltage of 10 kV and a beam current of 0.14 nA. The SEM analysis of all the samples (pristine CuHCF and CuCHF powders coated with different amounts of PEDOT:PSS) has been performed without using any additional sputtered conductive material.

The X-ray powder diffraction (XRPD) patterns were recorded using a Miniflex Rigaku® diffractometer, utilizing CuK α radiation at

ambient temperature, scanning a 2θ range of $10\text{--}60^\circ$ with a scan speed of 5 seconds per step and a step width of 0.03° . The powder sample was held in a quartz holder without the need for any solvent. Diffractograms were normalized according to the maximum peak intensity.

Electrochemical Measurements

All the electrochemical measurements were conducted using a BioLogic VMP3 instrument in a three-electrode cell configuration (half-cell) with a CuHCF-based working electrode and two zinc foils ($150\text{ }\mu\text{m}$ thickness, 99.95%, Good Fellow) as counter and reference electrodes, with a 100 mM ZnSO_4 electrolyte solution (Heptahydrate, 99.995%, Sigma Aldrich). The working electrode was made by brushing a CuHCF-based slurry onto a carbon cloth (Fuel Cell Earth) current collector with a mass loading of the active material of 10 mg cm^{-2} . The slurry was made by mixing CuHCF or CuHCF/PEDOT:PSS powder, amorphous carbon (Super C65, Timcal), polyvinylidene fluoride (PVdF) (Solef S5130, Solvay), and graphite (SFG6, Timcal) with N-methyl-2-pyrrolidone (NMP) in a ratio of 80:9:9:2, dispersed for 30 min at 4000 rpm using an IKA T10 Ultra-Turrax. Before cell assembly, the working electrode was annealed at 100° for 6 hours in a vacuum oven.

In order to ensure the electrochemical stability of the coating polymer within the designated voltage window, cyclic voltammetry (CV) experiments were conducted using electrodes containing both coated and uncoated active material in the as-assembled three-electrode electrochemical cells. The scan rate employed during the experiments was set at 0.1 mV s^{-1} . Before each electrochemical test, the open circuit potential was recorded for a minute.

2. Results and Discussion

Initially, as described within the experimental section, in-house synthesized CuHCF particles have been coated with different amounts of PEDOT:PSS, after being immersed in a water-based dispersion containing different amounts of polymer (namely: 2.5 wt.%, 4.5 wt.%, 8.5 wt.%, and 12.5 wt.%).

The morphology and the chemical composition of CuHCF particles were investigated before and after the addition of PEDOT:PSS through SEM coupled with EDS. As it can be seen in Figure 1, the SEM images of the CuHCF powders showed that the overall shape and the average size of the particles remained

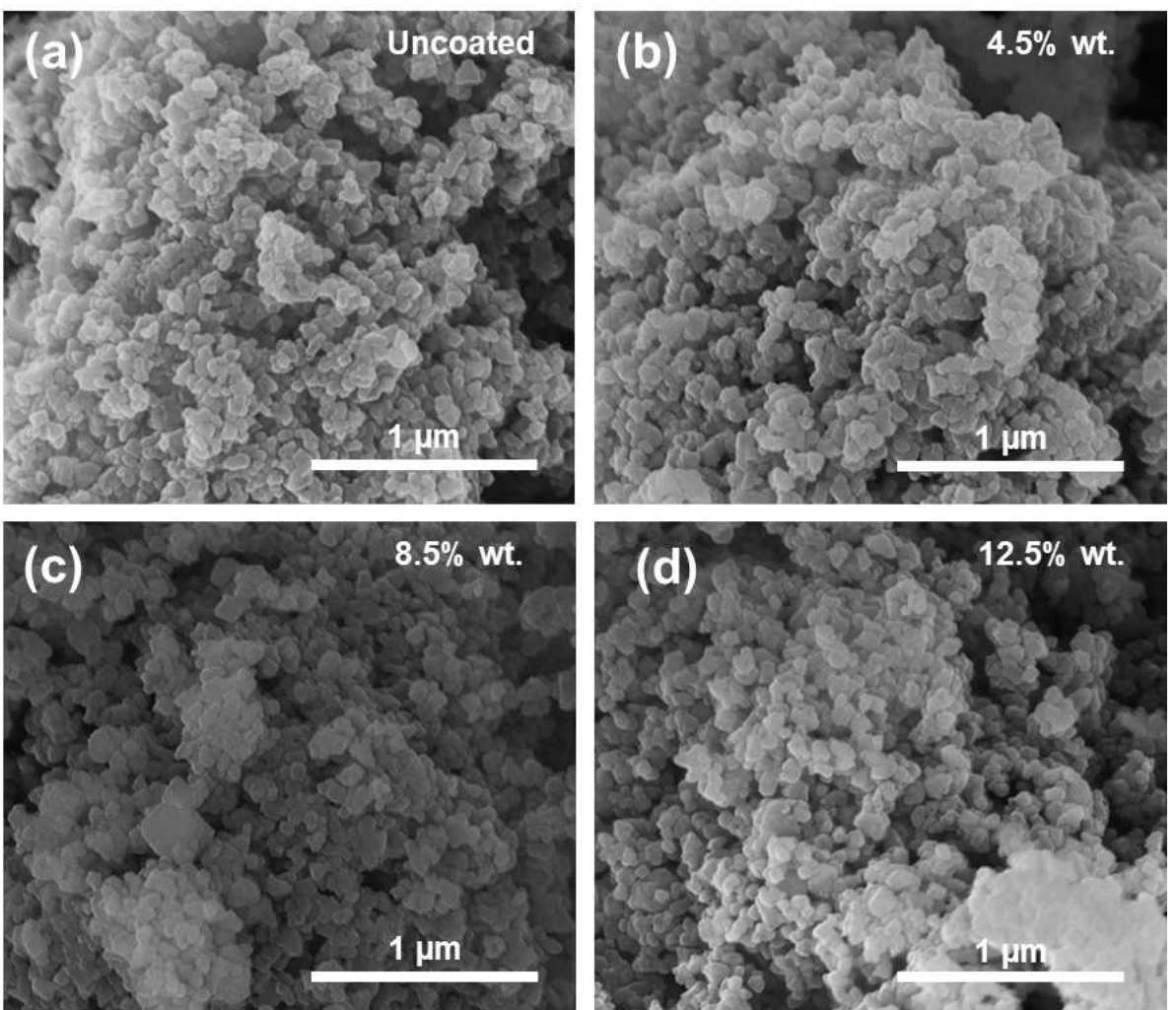


Figure 1. SEM images of (a) pristine uncoated CuHCF particles and coated CuHCF@PEDOT:PSS particles using dispersions containing a PEDOT:PSS concentration of (b) 4.5 wt.%, (c) 8.5 wt.%, and (d) 12.5 wt.%.

unchanged among all samples independently of the addition of the PEDOT:PSS.

The XRPD patterns (Supporting Information Section 1, Figure S1) demonstrated that the crystallinity and the unit size of CuHCF were not affected by the addition of PEDOT:PSS. Interestingly, this results suggests that no intercalation of the PEDOT:PSS occurs within the CuHCF structure, since if this were the case, the structural analysis would show an alteration of the crystallographic pattern of the material.^[26,55] Since PEDOT:PSS contains two sulfur atoms per unit monomer, the presence of the polymer on the surface of the coated CuHCF powders was confirmed using SEM-EDS through the identification of atomic sulfur, which is otherwise absent in the pristine CuHCF powder (Supporting Information Section 2, Figure S2).

It has been demonstrated in the literature that conductive polymers interact with batteries active materials mainly either through intercalating in the material's structure or through forming a coating onto its surface.^[26,55] As an example, the in situ polymerization of conductive monomers mixed with V₂O₅ led to an intercalation of the polymer into the material, as indicated by the increase in the interlayer spacing within the V₂O₅ crystal structure due to the growth of polymer chains inside it.^[26,55] In contrast, with materials such as MnO₂ or PBAs in particular when suspensions or dispersions of pre-polymerized polymers were used, the polymers tend to form a surface coating rather than intercalating into their structure.^[55] To the best of our knowledge, there are no reports suggesting the intercalation of conductive polymers into the crystal structure of PBAs, with multiple studies indicating a coating mechanism instead.^[55] Considering the findings discussed in the literature, and the results from both the structural (Figure S1 of the Supporting Information) and the compositional analysis (Figure S2 of the Supporting Information) it is most likely that the PEDOT:PSS forms a coating onto the CuHCF particles.

Moreover, the analysis of several SEM-EDS mappings showed that the amount of detected sulfur in the coated CuHCF@PEDOT:PSS particles increased with the increasing concentration of PEDOT:PSS in the coating dispersion. In particular, as summarized in Figure 2, the atomic percentage of sulfur detected onto the coated CuHCF@PEDOT:PSS powders increased sharply until the amount of polymer within the initial dispersion solution reached 8.5 wt.%, and then it remained mostly constant, suggesting a saturation of the maximum amount of polymer that could be added onto the CuHCF particles.

It is essential to notice that the specific behavior of PEDOT:PSS and its interaction with the surface of the active material may depend on various factors, including the formulation of the coating dispersion, the nature of the sample surface, and the coating process parameters.^[6,26,41,55] A potential reason for the saturation of the sulfur amount observed in Figure 2 could be that the critical micelle concentration of the CuHCF/PEDOT:PSS mixture is exceeded once the concentration of the PEDOT:PSS within the coating dispersion reaches 8.5 wt.%. If the critical micelle concentration is exceeded, it is likely that the excess polymer molecules self-assemble into micelles, on one side stabilizing the polymeric dispersion while on the other side preventing any further precipitation of PEDOT:PSS on the sample surface during the coating process. This could result in relatively non-uniform deposition of PEDOT:PSS on the surface of the CuHCF particles as suggested by SEM-EDS images of the CuHCF@PEDOT:PSS 12.5 wt.% sample (Supporting Information Section 2, Figure S2).

The electrochemical stability of the coated CuHCF@PEDOT:PSS was evaluated through cyclic voltammetry recorded with a scan rate of 0.1 mV s⁻¹ between 1.25 V and 2.15 V vs. Zn²⁺/Zn in an aqueous 100 mM ZnSO₄ electrolyte (Figure 3). It is worth noticing that when CuHCF is polarized within this

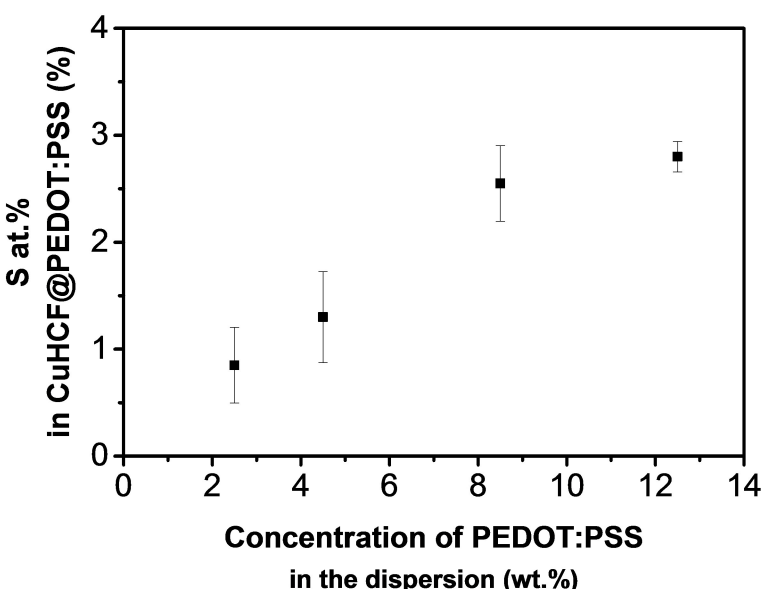


Figure 2. Average atomic percentage of sulfur on the surface of the uncoated CuHCF and of all the coated CuHCF@PEDOT:PSS powders detected from the SEM-EDS measurements as a function of the amount of PEDOT:PSS added within the coating dispersion. The mean values and standard deviations have been averaged from at least three different compositional mappings per type of sample belonging to different preparation batches.

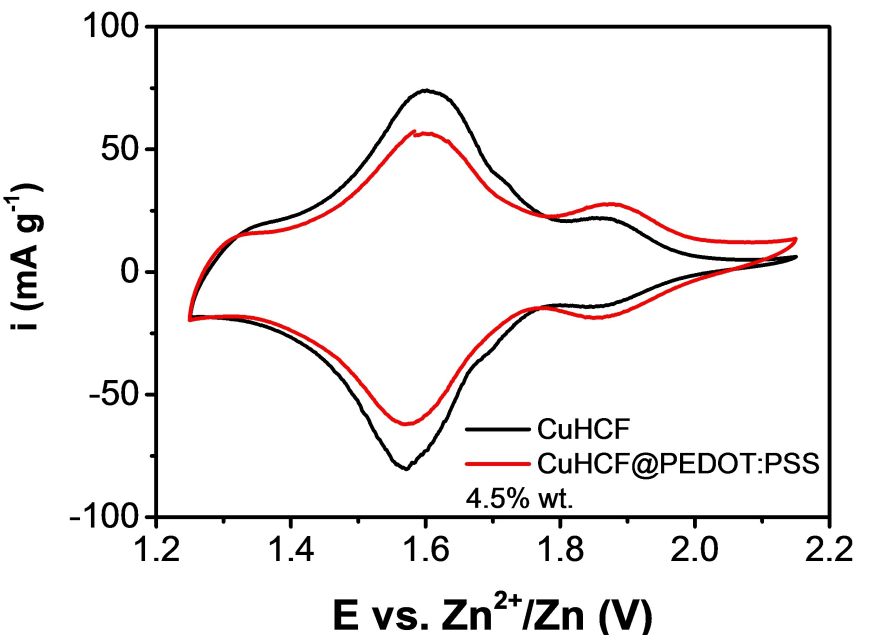


Figure 3. Cyclic voltammetry of the CuHCF-based electrode uncoated (black line) and coated with 4.5 wt. % of PEDOT:PSS (red line). The voltammograms have been measured with a scan rate of 0.1 mV s^{-1} between 1.25 V and 2.15 V vs. Zn^{2+}/Zn in an aqueous solution containing $100 \text{ mM} \text{ ZnSO}_4$.

potential window no oxidation/reduction of the water solution containing ZnSO_4 occurs.^[4,7,8,13,15–17,19,64] As shown in Figure 3, the voltammogram of the coated CuHCF@PEDOT:PSS retained the same electrochemical behavior of the uncoated CuHCF. Upon coating CuHCF with PEDOT:PSS, the peaks of the voltammogram maintained their position in terms of potential, indicating that the presence of the polymer does not interfere with the insertion/deinsertion of Zn^{2+} in/from CuHCF. Moreover, no additional irreversible peak appeared during the cycling of the coated CuHCF@PEDOT:PSS suggesting that the PEDOT:PSS is stable in the potential range chosen for the experiment and in the slightly acidic Zn^{2+} -containing aqueous electrolyte ($\text{pH}=5.5$).

The charge/discharge performance of the coated CuHCF@-PEDOT:PSS electrodes was evaluated by galvanostatic cycling performed at a C-rate of 1 C (ca. 0.1 A g^{-1}) between 1.25 V and 2.15 V vs. Zn^{2+}/Zn in an aqueous electrolyte containing $100 \text{ mM} \text{ ZnSO}_4$. It is worth noticing that such C-rate has been chosen since it represents well the operating regime required for the batteries coupled with a stationary power grid.^[2] Moreover, assessing the cycle life of a material at a C-rate $> 10 \text{ C}$ produces misleading results in terms of apparently longer cycle life as it underestimates the degradation processes occurring in the materials, which depend on time rather than the cycles number.^[5] In fact, it is generally known that the higher the current rate, the slower the aging processes of an insertion material.^[5]

Figure 4 and Figure S3 (Supporting Information Section 3) illustrate the potential profiles of selected cycles of the uncoated CuHCF electrodes and of the CuHCF@PEDOT:PSS coated with different amounts of PEDOT:PSS. In all cases, the initial Zn^{2+} (de-)insertion takes place at a potential of ca. 1.6 V

vs. Zn^{2+}/Zn , which is associated with the $\text{Fe}^{\text{III}}/\text{Fe}^{\text{II}}$ redox couple present within the copper hexacyanoferrate lattice. However, during cycling, the Zn^{2+} (de-)insertion potential shifts towards higher values of ca. 1.75 V vs. Zn^{2+}/Zn , as seen from the plateau appearing in the galvanostatic profile. Such plateau at higher potentials is caused by a two-phase transition of the material, as already reported in the literature.^[4,7,8,13,17–19] Indeed detailed XRD analysis performed at different states of charge of CuHCF when cycled in a Zn^{2+} -containing aqueous electrolyte^[17] demonstrated the formation of new secondary phases in which the Cu^{2+} was substituted by Zn^{2+} , during the Zn^{2+} insertion. Since the post mortem diffraction pattern of the CuHCF did not match exactly the XRD pattern of ZnHCF phases, it was suggested that CuHCF converts to an unknown Zn-based distorted phase, in which Zn^{2+} or Cu^{2+} are partially substituting $\text{Fe}^{2+/3+}$ in the B sites of the material's lattice.^[17]

This behavior can be visualized more clearly with the aid of the differential charge plots shown in Figure 5 and Figure S4 (Supporting Information Section 4), where two pairs of peaks can be observed at ca. 1.6 V and at ca. 1.75 V vs. Zn^{2+}/Zn . The first pair of peaks at ca. 1.6 V vs. Zn^{2+}/Zn is present from the first cycle for all electrodes, while the second pair of peaks located at ca. 1.75 V vs. Zn^{2+}/Zn develops later during cycling. The first pair of peaks corresponds to the $\text{Fe}^{\text{III}}/\text{Fe}^{\text{II}}$ redox couple associated with the Zn^{2+} (de-)insertion. The second pair of peaks is correlated with the developing plateau at around the same potential observed in the galvanostatic profiles. The appearance of this plateau has been attributed to the transformation of CuHCF in a distorted form of Zinc hexacyanoferrate.^[18]

In the case of the uncoated CuHCF electrodes, the second pair of peaks at a higher potential of 1.75 V vs. Zn^{2+}/Zn appears

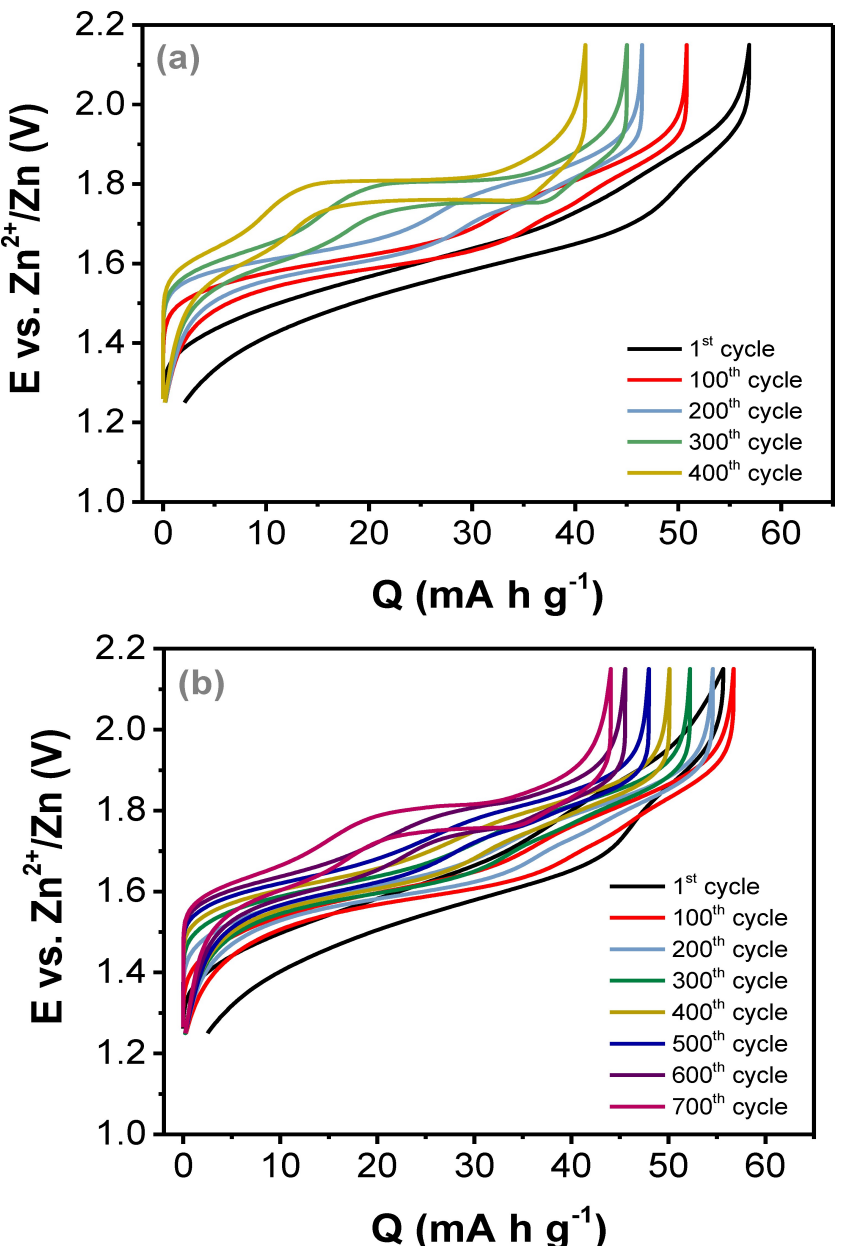


Figure 4. Galvanostatic cycles of the CuHCF electrode (a) uncoated and (b) coated with 4.5 wt.% PEDOT:PSS, recorded at a C-rate of 1 C in an aqueous solution containing 100 mM ZnSO_4 .

after ca. 200 cycles, in agreement with previous reports^[7,13,15] (Figure 5a). On the other side, as it can be seen in Figure 5b and Figure S4 (Supporting Information Section 4) when the CuHCF electrodes are coated with different amounts of PEDOT:PSS the pair of peaks located around 1.75 V vs. Zn^{2+}/Zn appears only after ca. 500 cycles. This delay in the appearance of the high potential peaks for the coated CuHCF@PEDOT:PSS suggests that the transformation of CuHCF in the distorted Zn hexacyanoferrate phase is considerably delayed during cycling due to the presence of the polymer, which appears to allow the initial crystal structure of the CuHCF to remain stable for a higher number of cycles.

It is worth mentioning that the sharpness and intensity of the peaks shown in the differential charge plots of the CuHCF@PEDOT:PSS samples (Figure 5b and Figure S4 of the Supporting Information Section 4) are related to the slope of the galvanostatic curve.^[65] In particular, the flatter the plateau in the galvanostatic cycle, the sharper the peak in the differential charge plot, as well as the higher its intensity.

In order to evaluate the effect of the presence of PEDOT:PSS on the cycle life of the CuHCF, the specific discharge capacity retention has been estimated at a current rate of 1 C (ca. 0.1 A g^{-1}) and shown in Figure 6.

All samples exhibited an initial specific discharge capacity ($Q_{\text{dis},0}$) ranging from 51 mAh g^{-1} to 57 mAh g^{-1} and an open

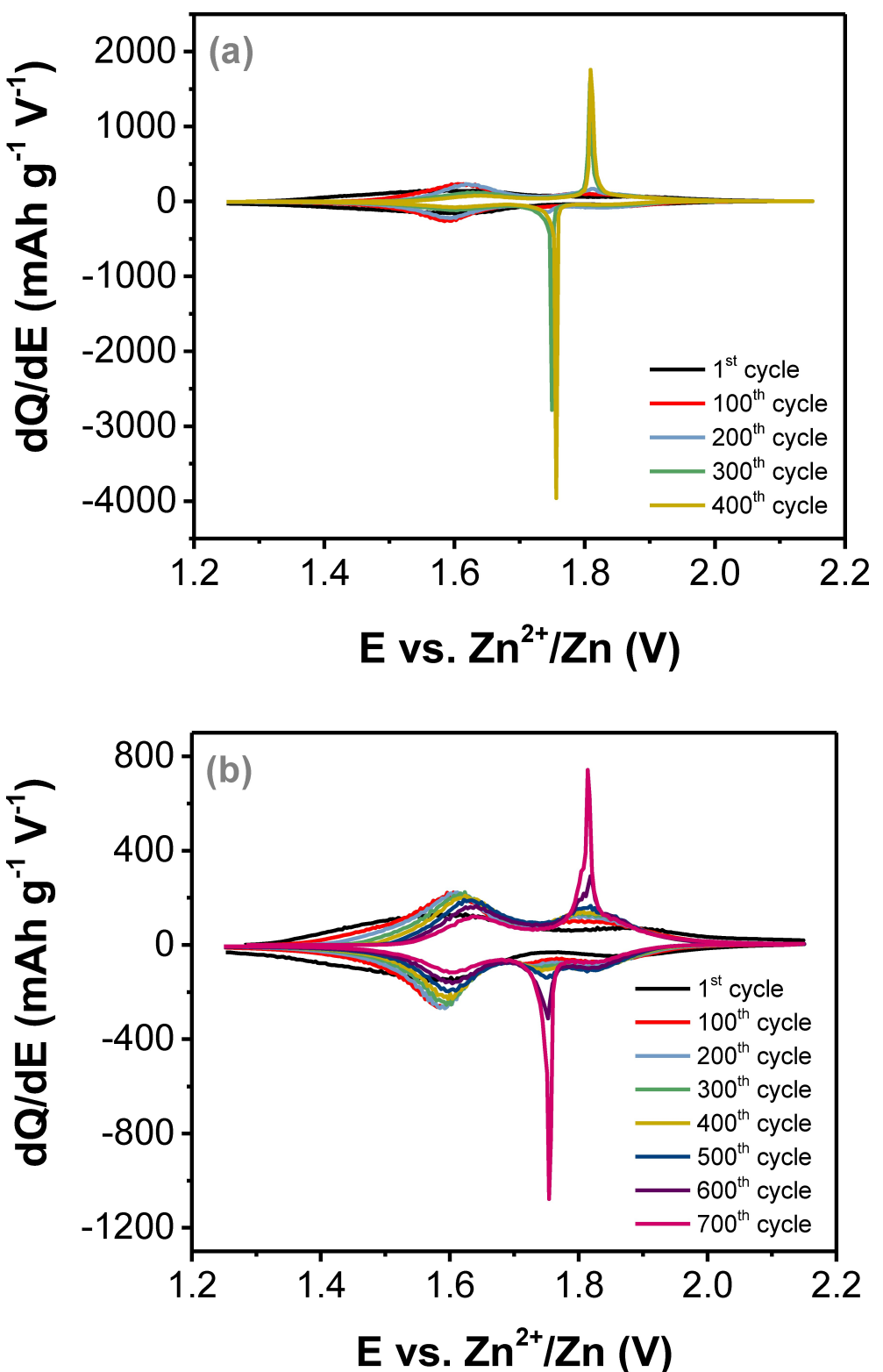


Figure 5. Differential charge plots of the CuHCF electrode (a) uncoated and (b) coated with 4.5 wt.% PEDOT:PSS, recorded at a C-rate of 1 C in an aqueous solution containing 100 mM ZnSO₄.

circuit potential (OCP) of ca. 1.6 V vs. Zn²⁺/Zn, as summarized in Table 1. Interestingly, as shown in Figure 6a, all the coated CuHCF@PEDOT:PSS electrodes displayed an activation phase for the first ~40 cycles, during which the specific capacity

increased up to a maximum value higher than the initial specific capacity, as summarized in Table 1. Such activation phase during the initial cycles of the coated active materials is a typical behavior when conductive polymers are used as coat-

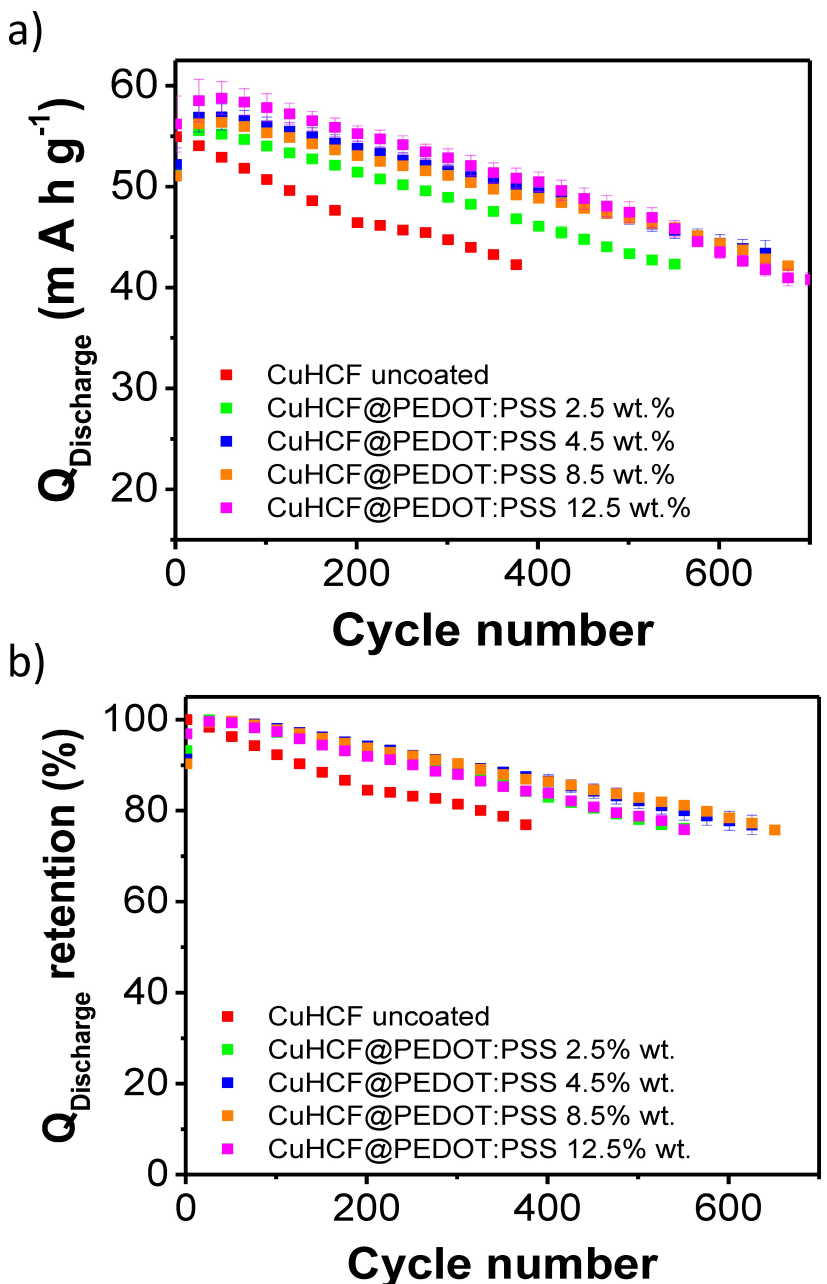


Figure 6. a) Average specific discharge capacity and b) average discharge retention of the synthesized CuHCF-based electrodes uncoated and coated with different amounts of PEDOT:PSS galvanostatically cycled at 1 C. Mean values and standard deviations have been obtained averaging at least three different measurements.

ings, and it is likely to be caused by the activation of the redox sites of the polymer and by the wetting of the ion pathways inside the polymeric coating itself.^[6,41,56] In particular, the experimental results summarized in Table 1 showed that the value of the specific discharge capacity at the 40th cycle ($Q_{\text{dis},40}$), namely after the activation of the polymer, slightly increased when the CuHCF was coated with the polymer. This demonstrates that the presence of PEDOT:PSS neither limited the active reaction surface area nor negatively affected the discharge capacity of the electrodes.

Figure 6b shows that coating the CuHCF particles with PEDOT:PSS significantly improved the cycle life of the electrode

by increasing the polymer concentration in the CuHCF/PEDOT:PSS coating dispersion up to 8.5 wt.%. However, the cycle life slightly shortened when the CuHCF particles were coated using a higher concentration of the polymer in the range of 12.5 wt.%. The 4.5% wt. and 8.5% wt. PEDOT:PSS-coated electrodes retained 80% of their initial specific discharge capacity after ca. 600 cycles, while the 12.5% wt. coated electrode exhibited a shorter lifespan of ca. 500 cycles, and the uncoated CuHCF electrode reached the same capacity retention only after ca. 350 cycles.

The CuHCF electrodes also retained different amounts of specific discharge energy during the cycling (Figure 7). Similar

Table 1. Initial specific discharge capacity, specific discharge capacity after 40 cycles, initial specific discharge energy, and open circuit potential of all the PEDOT:PSS coated and uncoated CuHCF-based electrodes. Mean values and standard deviations have been obtained by averaging at the values collected from more than three different measurements.

Concentration of polymer in CuHCF/PEDOT: PSS dispersion (wt.%)	$Q_{\text{dis},0}$ (mAh.g ⁻¹)	$Q_{\text{dis},40}$ (mAh.g ⁻¹)	$E_{\text{dis},40}$ (mWh.g ⁻¹)	OCP (V)
0.0% (Uncoated)	54.9 ± 0.2	53.6 ± 0.2	86.8 ± 0.2	1.62
2.5%	51.8 ± 0.5	55.5 ± 0.3	89.7 ± 0.3	1.58
4.5%	52.2 ± 1.6	57.0 ± 1.3	91.2 ± 1.6	1.60
8.5%	51.1 ± 0.0	56.5 ± 0.3	90.1 ± 0.4	1.61
12.5%	56.2 ± 2.7	57.3 ± 0.8	91.6 ± 0.9	1.64

to the discharge capacity retention, the CuHCF-based electrode coated with 4.5 wt.% of PEDOT:PSS presented the best discharge energy retention, reaching 80% after ca. 700 cycles, compared to the uncoated electrode, whose energy cycle life was only ca. 400 cycles. In all cases, the cycle life was extended when considering the average specific energy of the electrode compared to the electrode's discharge capacity due to the phase transition occurring upon cycling the CuHCF. As already explained in the previous paragraphs and as reported in,^[4,7,8,13,17–19] the two-phase transition of the CuHCF over prolonged cycling in Zn-containing aqueous electrolytes provokes the increase of the Zn²⁺ intercalation potential, which in turns allows for higher discharge energies. The already

discussed phase transformation thus, with the increase of the Zn²⁺ intercalation potential, partially compensates the effect of the material's aging resulting in the slow decrease of its discharge capacity.^[4,7,8,13,17–19]

Such improvement in the cycle life of the CuHCF when coated with PEDOT:PSS has been obtained in relevant cycling conditions involving a current rate of 1 C (ca. 0.1 A g⁻¹) and electrodes having a high active material mass loading (10 mg cm⁻²). Such experimental conditions, although application-relevant, are rarely used in the A-ZIBs literature, where the majority of the experimental results are obtained with mass loadings of the electrodes $\leq 2 \text{ mg cm}^{-2}$ and C-rates $\geq 10 \text{ C}$.^[2,5]

The observed slightly shorter cycle life of the CuHCF@PEDOT:PSS when using a PEDOT:PSS coating dispersion with a polymer concentration higher than 8.5 wt.% could be attributed to several potential reasons. What we consider the most probable is that the polymer particles may aggregate rather than adhere to the surface of the active material when the critical micelle concentration of the coating dispersion is reached, and this may happen for dispersions containing a concentration of PEDOT:PSS $> 8.5 \text{ wt. \%, as suggested by Figure 2}$. The likely aggregation of the polymer particles in the coating dispersion may lead to non-uniform charge/discharge reactions and uneven distribution of mechanical stress/strain within the electrode, with relative increase in material loss, or to uneven mechanical properties of the electrode. This can cause formation of cracks, delamination, and loss of adhesion of the positive electrode material, which in turn can accelerate the degradation of the electrode and shorten its cycle life.

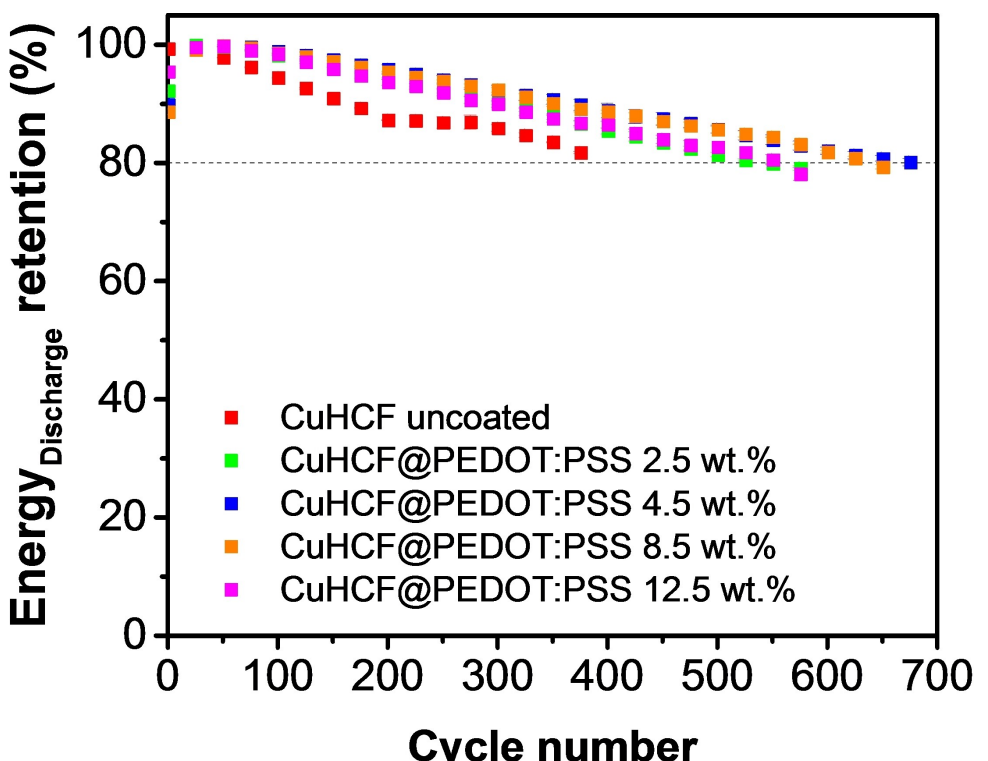


Figure 7. Average discharge energy retention of the synthesized CuHCF-based electrodes uncoated and coated with different amounts of PEDOT:PSS galvanostatically cycled at 1 C. Mean values and standard deviations have been obtained, averaging at least three measurements.

Figure 8a shows that all CuHCF@PEDOT:PSS electrodes demonstrated very high coulombic efficiencies all $\geq 99.5\%$ and very high-rate capabilities, regardless of the presence and of the amount of PEDOT:PSS coating. The power rate capability of the uncoated CuHCF electrodes and of the coated CuHCF@PEDOT:PSS electrodes is shown in Figure 8b.

In order to compare meaningfully the power rate capability of the uncoated CuHCF with the coated CuHCF@PEDOT:PSS electrodes, the power test has been recorded after the activation phase occurring during the initial galvanostatic cycles of the CuHCF@PEDOT:PSS electrodes showed in the previous paragraphs. The power-rate test has been performed starting

with a current rate of 1 C (ca. 0.1 A g^{-1}) followed by current rates of 2 C (ca. 0.2 A g^{-1}), 5 C (ca. 0.5 A g^{-1}), 10 C (ca. 1 A g^{-1}), and 1 C (ca. 0.1 A g^{-1}). As reported in Figure 8b, the CuHCF@PEDOT:PSS electrodes retained their initial specific discharge capacity regardless of the amount of polymer in the coating, indicating once again that the presence of the PEDOT:PSS does not affect negatively the power performance of the material.

Lastly, the performance of the CuHCF@PEDOT:PSS coated with 4.5 wt.% of PEDOT:PSS has been compared with the results already published in the literature, where active materials for aqueous Zn-ion batteries were coated/mixed with different polymers to improve their cycle life. Due to the

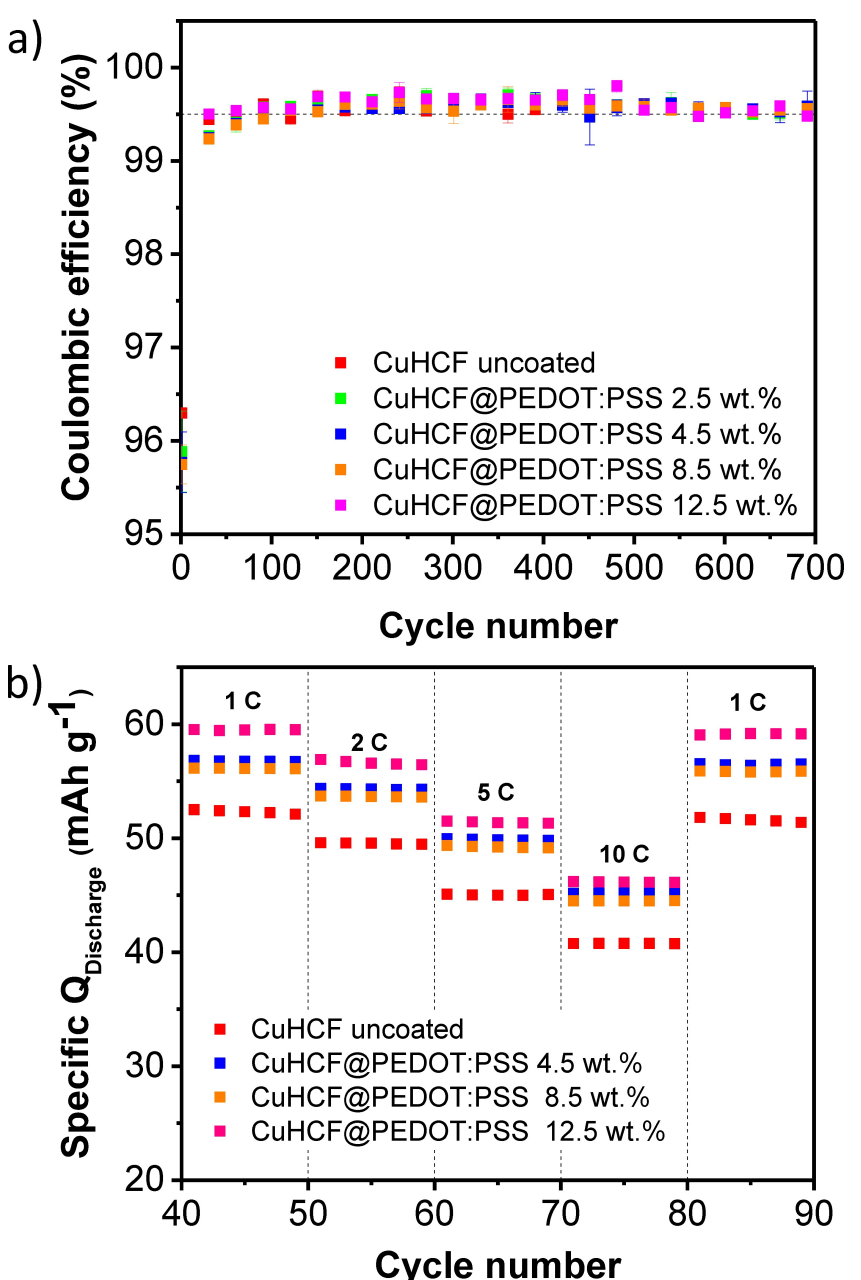


Figure 8. a) Average value of coulombic efficiency of the synthesized CuHCF-based electrodes, coated with various amounts of PEDOT:PSS and galvanostatically cycled at 1 C. Mean values and standard deviations have been obtained averaging at least three measurements. b) Galvanostatic power test of uncoated CuHCF and coated CuHCF@PEDOT:PSS electrodes with different amount of PEDOT:PSS in the coating.

Table 2. Comparison of the results reported in the literature on the effect of polymeric coatings on the performance of different active materials for aqueous Zn-ion batteries. Only the published results reporting a minimum resulting areal capacity of 0.5 mAh cm^{-2} have been considered for the comparison.

Polymer	Active material	Areal capacity (mAh cm^{-2})	Actual C-rate	Cycle life	Normalized Cycle Life C-Life/C-rate	Ref.
PANI	V_2O_5	0.98	25.6	100*	500	[59]
PEDOT:PSS	CuHCF	0.57	1.5	700	400	This work
PANI	V_2O_5	0.52	7.7	2000*	260	[60]
PANI	V_2O_5	1.50	3.3	700	210	[61]
PANI	V_2O_5	0.6	0.3	30	100	[34]
PEDOT	V_2O_5	0.70	2.8	100*	35	[62]
PEDOT:PSS	V_2O_5	1.05	16.6	100	6	[63]

*Longer cycle life not assessed.

relatively little number of reports, not only the research works involving PBAs as active materials coated with PEDOT:PSS were considered for the comparison. In fact, all the active materials for aqueous Zn-ion batteries that were coated/mixed with different polymers (PEDOT, PEDOT:PSS, PANI and PPy) were included in the comparison. To offer a meaningful comparison of the published results, relevant parameters such as areal capacity, actual C-rate (obtained at the current employed for the cycle life assessment considering the experimental specific capacity), cycle life and normalized cycle life with respect to the C-rate employed during the cycle life assessment have been considered. The complete comparison of the results published in the literature with other parameters such as mass loading, specific current used for the cycle life assessment, etc. can be found within the Supporting Information Section 5.

This last parameter (normalized cycle life with respect to the C-rate) has been taken into account since the phenomena responsible for the aging of the battery electrode materials are strongly dependent on the current rate employed during the measurement. It has been shown that the higher the current rate of the experiments, the longer the cycle life of the material,^[19,57, 58] because the aging processes are often related to the time rather than to the number of cycles itself, and high current rates allow for a higher number of cycle per unit time.^[19,57, 58] The experimental conditions in which the cycle life of an electrode for aqueous Zn-ion battery should be assessed is around 1 C, as it is dictated from the power grid application.^[2] To the best of our knowledge, only 22% of the published papers (i.e. 6 papers out of the 27 reviewed, including this one) reported the cycle life assessment of the polymer coated/intercalated aqueous Zn-ion battery materials at a relevant C-rate for the stationary applications, namely $0.5 \leq \text{C-rate} \leq 5$ (Table 2 and Table S1, S2, S3), and none of them reports the reproducibility of the results and the error bars. Considering this lack of standardization of the current chosen for the cycle life assessment of the Zn-ion battery materials, without considering a cycle life normalized to the C rate it would be impossible to compare the different cycle lives reported in the literature.

As shown in Table 2, the CuHCF@PEDOT:PSS with 4.5 wt. % of PEDOT:PSS showed the second best performance overall in terms of cycle life normalized for the C rate and the best results for the Prussian blue analogues active materials when coated with a polymer. Other literature reports have been published, however they have not been taken into account for the comparison because of the resulting poor areal capacity $< 0.5 \text{ mAh cm}^{-2}$, which is too low to be interesting from a real-life application point of view. These published works are shown in Table S2 in the Supporting Information Section 5. Moreover, it was found that, to the best of our knowledge, 33% of the published manuscripts (9 out of 27) did not report any information on the mass loading of the electrodes used for the cycle life assessment. Such reports have not been considered for the comparison since information about the mass loading of the electrodes used to produce the results are missing. Not only this is a poor scientific practice, but also this makes the assessment of the reported performance non-relevant for comparisons. Such reports are summarized in Table S3 in the Supporting Information Section 5.

3. Conclusions

In this study the use of conductive PEDOT:PSS as a coating of CuHCF-based electrodes for aqueous Zn-ion batteries was investigated. The compositional analysis of the polymer-coated samples revealed that the amount of PEDOT:PSS on the surface of the active material particles increased with increasing the polymer concentration in the coating dispersion up to 8.5 wt. %. However, beyond this concentration the amount of polymer detected onto the surface of the CuHCF particles remained constant, suggesting an aggregation of the polymeric coating. Cyclic voltammetry analysis on the coated CuHCF@PEDOT:PSS demonstrated the electrochemical stability of the polymer in the potential range necessary of the (de-)insertion of Zn^{2+} (from)in the material as well as no interference with its Zn^{2+} intercalation kinetics.

Galvanostatic cycling showed that the cycle life of CuHCF was significantly enhanced using PEDOT:PSS when a coating

dispersion with a polymer concentrations up to 8.5 wt.% was used. In this case, the CuHCF@PEDOT:PSS retained 80% of its initial discharge energy for ca. 700 cycles at a current rate of 1 C, compared to the uncoated sample reaching only ca. 400 cycles. Based on our results, a PEDOT:PSS dispersion concentration of 4.5 wt.% resulted optimal, as the CuHCF@PEDOT:PSS achieved the best electrochemical performance while needing lower amounts of the polymer.

Moreover, all the CuHCF@PEDOT:PSS exhibited a very high Coulombic efficiency ($\geq 99.5\%$) and an excellent power rate capability, regardless of the amount of polymer. The improvement in the cycle life of the CuHCF when coated with PEDOT:PSS has been obtained in relevant cycling conditions involving not only a current rate of 1 C (i.e. 0.1 A g^{-1}), but also electrodes having a high active material mass loading (10 mg cm^{-2}). Such experimental conditions, although application-relevant, are rarely used in the aqueous ZIB literature, where the majority of the experimental results are obtained with mass loadings of the active material in the electrodes $\leq 2 \text{ mg cm}^{-2}$ and C-rates $\geq 10 \text{ C}$.^[5] The comparison with other published reports showed that the CuHCF@PEDOT:PSS with 4.5 wt.% of PEDOT:PSS resulted in the second best performance overall in terms of cycle life normalized for the actual C-rate of the experiments and the best results for the Prussian blue analogues active materials when coated with a polymer.

Overall, our findings suggest that the PEDOT:PSS can be used as solid-state additive/coating in the electrode to effectively improve the electrochemical performance of CuHCF in aqueous ZIBs, in terms of cycle life and in delaying its phase transition during cycling, even in application-relevant experimental conditions (i.e. current rate of 1 C and high active material mass loading of the electrode of 10 mg cm^{-2}).

Considering the challenges that remain open in increasing the stability of CuHCF in the presence of Zn^{2+} ions, our study supports the use of conductive polymer coatings as a promising strategy to accelerate the commercialization of A-ZIBs. Further research should be addressed to optimize the use of conductive polymers for potential applications in the field of the aqueous Zn-ion technology.

Acknowledgements

The financial support of the Federal Ministry of Education and Research (BMBF) in the framework of the project "ZIB" (FKZ 03XP0204A) and in the frame of the project "ZIB2" (FKZ 03XP0523B) is gratefully acknowledged. Open Access funding enabled and organized by Projekt DEAL.

Conflict of Interests

The authors declare no conflict of interest.

Data Availability Statement

The data that support the findings of this study are available from the corresponding author upon reasonable request.

Keywords: Aqueous zinc-ion batteries (A-ZIBs) · Prussian blue analogues (PBAs) · Copper hexacyanoferrate (CuHCF) · Cycle life · Conductive polymer · PEDOT:PSS

- [1] Z. Yang, J. Zhang, M. C. W. Kintner-Meyer, X. Lu, D. Choi, J. P. Lemmon, J. Liu, *Chemical Reviews*, 2011, 111, 3577–3613.
- [2] H. C. Hesse, M. Schimpe, D. Kucevic, A. Jossen, *Energies* 2017, 10, 2107.
- [3] J. Shin, J. Lee, Y. Park, J. W. Choi, *Chem. Sci.* 2020, 11, 2028–2044.
- [4] G. Zampardi, F. La Mantia, *Curr. Opin. Electrochem.* 2020, 21, 84–92.
- [5] G. Zampardi, F. La Mantia, *Nat. Commun.* 2022, 13, 1–5.
- [6] D. S. Kim, H. Yoo, M. S. Park, H. Kim, *J. Alloys Compd.* 2019, 791, 385–390.
- [7] G. Kasiri, J. Glenneberg, R. Kun, G. Zampardi, F. La Mantia, *ChemElectroChem* 2020, 7 (15), 3301–3310.
- [8] G. Kasiri, J. Glenneberg, A. Bani Hashemi, R. Kun, F. La Mantia, *Energy Storage Mater.* 2019, 19, 360–369.
- [9] A. Widmann, H. Kahlert, H. Wulff, F. Scholz, *J. Solid State Electrochem.* 2005, 9, 380–389.
- [10] S. Kjeldgaard, M. Wagemaker, B. B. Iversen, A. Bentien, *Mater Adv* 2021, 2, 2036–2044.
- [11] N. Kuperman, A. Cairns, G. Goncher, R. Solanki, 2020, 362, 137077.
- [12] Z. Jia, B. Wang, Y. Wang, *Mater Chem Phys* 2015, 149–150, 601–606.
- [13] G. Zampardi, M. Warnecke, M. Tribbia, J. Glenneberg, C. Santos, F. La Mantia, *Electrochim. Commun.* 2021, 126, 107030.
- [14] T. Gupta, A. Kim, S. Phadke, S. Biswas, T. Luong, B. J. Hertzberg, M. Chamoun, K. Evans-Lutterodt, D. A. Steingart, *J. Power Sources* 2016, 305, 22–29.
- [15] M. Baghodrat, G. Zampardi, J. Glenneberg, F. La Mantia, *Batteries* 2023, 9 (3), 170.
- [16] M. Tribbia, G. Zampardi, F. La Mantia, *Curr Opin Electrochem* 2023, 38, 101230.
- [17] R. Trócoli, G. Kasiri, F. La Mantia, *J. Power Sources* 2018, 400, 167–171.
- [18] J. Lim, G. Kasiri, R. Sahu, K. Schweinar, K. Hengge, D. Raabe, F. La Mantia, C. Scheu, *Chem. Eur. J.* 2020, 26, 4917–4922.
- [19] G. Kasiri, R. Trócoli, A. Bani Hashemi, F. La Mantia, *Electrochim. Acta* 2016, 222, 74–83.
- [20] V. Renman, D. O. Ojwang, M. Valvo, C. P. Gómez, T. Gustafsson, G. Svensson, *J. Power Sources* 2017, 369, 146–153.
- [21] M. Görlin, D. O. Ojwang, M. T. Lee, V. Renman, C. W. Tai, M. Valvo, *ACS Appl. Mater. Interfaces* 2021, 13, 59962–59974.
- [22] D. O. Ojwang, J. Grins, D. Wardecki, M. Valvo, V. Renman, L. Häggström, T. Ericsson, T. Gustafsson, A. Mahmoud, R. P. Hermann, G. Svensson, *Inorg. Chem.* 2016, 55, 5924–5934.
- [23] Q. Xue, L. Li, Y. Huang, R. Huang, F. Wu, R. Chen, *ACS Appl Mater Interfaces* 2019, 11, 22339–22345.
- [24] B. Wang, S. Dai, Z. Zhu, L. Hu, Z. Su, Y. Jin, L. Xiong, J. Gao, J. Wan, Z. Li, L. Huang, *Nanoscale* 2022, 14, 12013–12021.
- [25] E. G. Tolstopiatova, M. A. Kamenskii, V. V. Kondratiev, *Energies* 2022, 15, 8966.
- [26] G. He, Y. Liu, D. E. Gray, J. Othon, *Composites Communications*. 2021, 27, 100882.
- [27] F. Wu, J. Liu, L. Li, X. Zhang, R. Luo, Y. Ye, R. Chen, *ACS Appl. Mater. Interfaces* 2016, 8, 23095–23104.
- [28] W. J. Li, S. L. Chou, J. Z. Wang, J. L. Wang, Q. F. Gu, H. K. Liu, S. X. Dou, *Nano Energy* 2015, 13, 200–207.
- [29] J. Mao, F. F. Wu, W. H. Shi, W. X. Liu, X. L. Xu, G. F. Cai, Y. W. Li, X. H. Cao, *Chinese Journal of Polymer Science (English Edition)* 2020, 38, 514–521.
- [30] Y. Du, Y. Chen, M. Yang, S. Zou, X. Song, Y. Fu, J. Li, Y. Li, D. He, *ACS Appl. Energ. Mater.* 2021, 4, 14582–14589.
- [31] S. F. Hong, L. C. A. Chen, *Electrochim. Acta* 2010, 55, 3966–3973.
- [32] Q. Sun, L. Chang, Y. Liu, W. Nie, T. Duan, Q. Xu, H. Cheng, X. Lu, *ACS Appl Energy Mater* 2023, 6, 3102–3112.
- [33] Y. Tang, W. Zhang, L. Xue, X. Ding, T. Wang, X. Liu, J. Liu, X. Li, Y. Huang, *J Mater Chem A Mater* 2016, 4, 6036–6041.
- [34] Y. Zhang, L. Xu, H. Jiang, Y. Liu, C. Meng, *J. Colloid Interface Sci.* 2021, 603, 641–650.

- [35] Z. Zhang, B. Xi, X. Wang, X. Ma, W. Chen, J. Feng, S. Xiong, *Adv Funct Mater* **2021**, *31*, 2103070.
- [36] Y. Zhang, X. Lin, X. Tang, K. Hu, X. Lin, G. Xie, X. Liu, H. J. Qiu, *ACS Appl. Nano Mater.* **2022**, *5*, 12729–12736.
- [37] Q. Liu, Z. Ma, Z. Chen, M. Cui, H. Lei, J. Wang, J. B. Fei, N. He, Y. Liu, Q. Liu, W. Li, Y. Huang, *Chem. Commun.* **2022**, *58*, 8226–8229.
- [38] J. W. Xu, Q. L. Gao, Y. M. Xia, X. Lin, X. Sen, W. L. Liu, M. M. Ren, F. G. Kong, S. J. Wang, C. Lin, *J. Colloid Interface Sci.* **2021**, *598*, 419–429.
- [39] M. A. Kamenskii, F. S. Volkov, S. N. Eliseeva, R. Holze, V. V. Kondratiev, *J. Electrochem. Soc.* **2023**, *170*, 010505.
- [40] K. Sun, S. Zhang, P. Li, Y. Xia, X. Zhang, D. Du, F. H. Isikgor, J. Ouyang, *Journal of Materials Science: Materials in Electronics.* **2015**, *26*, 4438–4462.
- [41] L. Xu, J. Ma, P. Guo, C. Su, *Nano* **2019**, *14*, 1950116.
- [42] Y. Liu, L. Xie, W. Zhang, Z. Dai, W. Wei, S. Luo, X. Chen, W. Chen, F. Rao, L. Wang, Y. Huang, *ACS Appl. Mater. Interfaces* **2019**, *11*, 30943–30952.
- [43] S. Bai, Y. Ma, X. Jiang, Q. Li, Z. Yang, Q. Liu, D. He, *Surfaces and Interfaces* **2017**, *8*, 214–218.
- [44] L. Hu, J. Song, X. Yin, Z. Su, Z. Li, *Polymers* **2020**, *12*, 145.
- [45] P. R. Das, L. Komsiyska, O. Ostros, Wittstock, *J. Electrochem. Soc.* **2015**, *162*, A674–A678.
- [46] C. Zhou, Z. Liu, X. Du, S. P. Ringer, *Synth. Met.* **2010**, *160*, 1636–1641.
- [47] D. H. Yoon, S. H. Yoon, K. S. Ryu, Y. J. Park, *Sci Rep* **2016**, *6*, 19962.
- [48] M. Eckert, W. Peters, J. F. Drillet, *Materials* **2018**, *11*, 2399.
- [49] J. F. Drillet, R. Dittmeyer, K. Jüttner, *J. Appl. Electrochem.* **2007**, *37*, 1219–1226.
- [50] J. F. Drillet, R. Dittmeyer, K. Jüttner, L. Li, K. M. Mangold, *Fuel Cells* **2006**, *6*, 432–438.
- [51] G. G. Láng, M. Ujvári, S. Vesztergom, V. Kondratiev, J. Gubicza, K. J. Szekeres, *The Electrochemical Degradation of Poly(3,4-Ethylenedioxythiophene) Films Electrodeposited from Aqueous Solutions* **2016**, *230*, 1281–1302.
- [52] K. Cai, S. Luo, L. hua Qian, X. Meng, S. xue Yan, J. Guo, Q. Wang, X. bing Ji, X. yan Zhou, *J. Power Sources* **2023**, *564*, 232854.
- [53] J. Lee, W. Choi, *J. Electrochem. Soc.* **2015**, *162*, A743–A748.
- [54] L. Stepien, A. Roch, R. Tkachov, B. Leupolt, L. Han, N. van Ngo, C. Leyens, *Synth. Met.* **2017**, *225*, 49–54.
- [55] P. Ruan, X. Xu, J. Feng, L. Yu, X. Gao, W. Shi, F. Wu, W. Liu, X. Zang, F. Ma, X. Cao, *Materials Research Bulletin* **2021**, *1*, 111077.
- [56] M. Chen, X. Li, Y. Yan, Y. Yang, Q. Xu, H. Liu, Y. Xia, *ACS Appl. Mater. Interfaces* **2022**, *14*, 1092–1101.
- [57] Y. Li, B. Liu, J. Ding, X. Han, Y. Deng, T. Wu, K. Amine, W. Hu, C. Zhong, J. Lu, *Batteries & Supercaps* **2020**, *4*, 60–71.
- [58] Z. Lin, T. Liu, X. Ai, C. Liang, *Nat. Commun.* **2018**, *9*, 5262.
- [59] Y. Zhang, Z. Li, M. Liu, J. Liu, *Chem. Eng. J.* **2023**, *463*, 142425.
- [60] J. Sun, Y. Zhao, Y. Liu, H. Jiang, D. Chen, L. Xu, T. Hu, C. Meng, Y. Zhang, *J. Colloid, Interface Sci.* **2023**, *633*, 923–931.
- [61] Q. Sun, L. Chang, Y. Liu, W. Nie, T. Duan, Q. Xu, H. Cheng, X. Lu, *ACS Appl. Energ. Mater.* **2023**, *6*, 3102–3112.
- [62] F. S. Volkov, E. G. Tolstopiatova, S. N. Eliseeva, M. A. Kamenskii, A. I. Vypritskaia, A. I. Volkov, V. V. Kondratiev, *Mater. Lett.* **2022**, *308*, 131210.
- [63] Y. Du, Y. Chen, M. Yang, S. Zou, X. Song, Y. Fu, J. Li, Y. Li, D. He, *ACS Appl. Energ. Mater.* **2021**, *4*, 14582–14589.
- [64] R. Trócoli, F. La Mantia, *ChemSusChem* **2014**, *8*, 481–485.
- [65] M. S. Palagonia, C. Erinmwingbovo, D. Brogioli, F. La Mantia, *J. Electroanal. Chem.* **2019**, *847*, 113170.

Manuscript received: March 5, 2024

Revised manuscript received: May 16, 2024

Accepted manuscript online: June 19, 2024

Version of record online: July 5, 2024